Title
Laboratory simulations of suprauroral mechanisms leading to perpendicular ion heating and conic formation

Journal
Journal of Geophysical Research, 96(A8)

ISSN
0148-0227

Authors
Sheehan, DP
Koslover, R
McWilliams, R

Publication Date
1991-08-01

DOI
10.1029/90ja02185

JOURNAL OF GEOPHYSICAL RESEARCH, VOL. 96, NO. A8, PAGES 14,107–14,118, AUGUST 1, 1991

Laboratory Simulations of Suprauroral Mechanisms Leading to Perpendicular Ion Heating and Conic Formation

D. P. SHEEHAN,[1] R. KOSLOVER,[2] AND R. MCWILLIAMS

Department of Physics, University of California, Irvine

Laboratory experiments are presented simulating aspects of perpendicular ion heating and conic formation that are observed or hypothesized to occur in the terrestrial ionosphere and magnetosphere. Previous laboratory observations of ion conics in the presence of the current-driven electrostatic ion cyclotron wave are reviewed. Field-aligned ion beams, accompanied by beam-generated electrostatic ion cyclotron modes, resulted in perpendicular energization of beam ions and also the heating of background plasma ions. Antenna-launched broadband and narrow-band lower hybrid waves produced considerable perpendicular ion heating and non-Maxwellian "tail" formation. Laboratory results are discussed in light of in situ measurements by the S3-3 satellite and the MARIE sounding rocket.

1. INTRODUCTION

This paper describes ongoing research in laboratory plasmas of phenomena that are known or hypothesized to occur in the terrestrial ionosphere and magnetosphere above the auroral oval. In particular, we focus on processes leading to perpendicular ion heating processes and some of the plasma conditions relevant to the formation of ion conics, upward flowing ion distributions exhibiting a preferred pitch angle in velocity space [*Gorney et al.*, 1981; *Horwitz*, 1980; *Ghielmetti et al.*, 1978; *Whalen et al.*, 1978; *Yau et al.*, 1983; *Shelley*, 1979]. Magnetospheric ions commonly are heated to over 100 times their initial temperatures perpendicularly to geomagnetic field lines. They have been observed by sounding rockets and satellites from 400-km to over 130,000-km altitude with variable compositions of H^+, O^+, and He^+. The mechanisms underlying the formation of ion conics have been the source of considerable theoretical research, and more than one mechanism has been proposed. Models usually require the existence of a low-altitude mechanism for causing ion energization or heating. This heating commonly is ascribed to electrostatic ion cyclotron waves (EICW), lower hybrid waves (LHW), narrow potential jumps [*Borovsky*, 1984], or some combination of these.

Electrostatic ion cyclotron waves may be generated by a net drift of the electron population [*Drummond and Rosenbluth*, 1962; *Rynn*, 1962; *Kindel and Kennel*, 1971] or by ion beams. EICW are expected to cause perpendicular ion heating in the suprauroral region [*Palmadesso et al.*, 1974; *Lysak et al.*, 1980; *Ashour-Abdalla et al.*, 1981] and have been observed to cause perpendicular ion heating in the laboratory [*Rynn et al.*, 1974]. EICW may be generated also by ion beams found in the suprauroral region [*Collin et al.*, 1981, 1984; *Richardson et al.*, 1981; *Miura et al.*, 1983; *Kaufmann and Kintner*, 1982, 1984; *Cattell et al.*, 1979; *Gorney et al.*, 1981, 1982]. Upward ion drifts have been correlated with suprauroral EICW [*Kintner et al.*, 1979; *Kintner*, 1980; *Cattell*, 1981; *Temerin et al.*, 1981] and EICW with ion heating [*Singh et al.*, 1981; *Singh and Schunk*, 1984; Kintner and Gorney, 1984]. In addition, EICW have been stimulated at low altitudes by man-made ion beams [*Jones*, 1981; *Kintner and Kelley*, 1981, 1982, 1983]. Theoretical and experimental studies of parallel and perpendicular ion beam injection into plasmas indicate that several electrostatic ion cyclotron modes may be destabilized and lead to ion acceleration and heating of beam and target plasma [*Perkins*, 1976; *Böhmer et al.*, 1976; *Hendel et al.*, 1976; *Hauck et al.*, 1978; *Yamada et al.*, 1977]. Reviews of proposed ion heating mechanisms are given by *Mozer et al.* [1980], *Kintner and Gorney* [1984], *Johnson* [1979], and *Lysak* [1986].

Following perpendicular heating at low altitudes, these transversely accelerated ions (TAI) may undergo adiabatic folding in the Earth's flaring magnetic field ($\mathbf{F} = -\mu\nabla\mathbf{B}$) leading to ion conics at higher altitudes. The motion of perpendicularly heated ions in a flaring magnetic field has been studied experimentally by *Cartier et al.*, [1985]. Interaction with double layers theoretically may also heat ions and generate ion conics [*Borovsky*, 1984]. The evolution of ion conics may be complicated by parallel electric fields [*Gorney et al.*, 1985].

TAIs and conics often are found loosely associated with plasma waves of various types, but unambiguous evidence of cause and effect relationships between them remains elusive. First, given the plethora of suprauroral waves, associations among them, TAIs, and conics is not surprising. Further, the transient nature of rocket and satellite measurements makes it difficult to follow ion evolution in the presence of waves. These problems are compounded by Doppler-shifting of waves due to rocket motion, difficulties in making wavelength measurements (usually only wave frequency is measured), or difficulties in discriminating between electrostatic and electromagnetic modes. In all, the expanse and complexity of the suprauroral region coupled with extreme experimental difficulties have conspired to limit understanding of conics, TAIs, and waves. Controlled laboratory experiments, therefore, may be useful in elucidating particular plasma processes.

This paper reviews and elaborates upon initial findings and presents new laboratory experiments simulating several ion acceleration and conic-forming mechanisms: electron-

[1]Permanently at Department of Physics, University of San Diego, San Diego, California.

[2]Permanently at Voss Scientific, Albuquerque, New Mexico.

Paper number 90JA02185.
0148-0227/91/90JA-02185$05.00

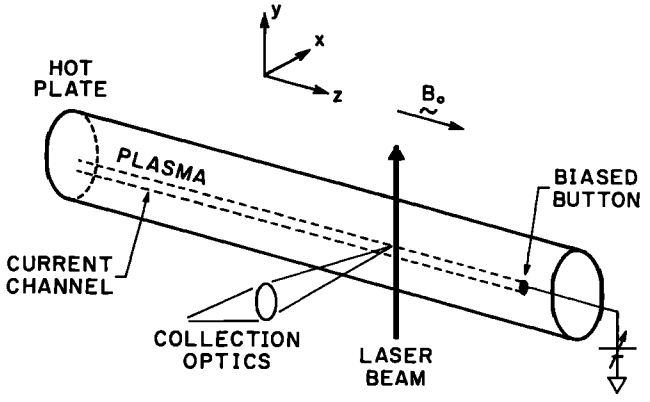

Fig. 1. Schematic for EICW experiment in electron-ion plasma depicting location of electron current channel in plasma, laser beam, and optics.

current-driven EICW, ion-beam-driven EICW, and lower hybrid wave heating. Comparisons between laboratory results and in situ measurements are made. The issue of adiabatic folding in flaring magnetic fields will not be addressed here.

2. Experimental Apparatus and Methods

These experiments were performed in the University of California, Irvine, Q machine [*Rynn and D'Angelo*, 1961; *Rynn*, 1964]. The cylindrical, flowing, steady state plasma (length, 1.2 m; diameter, 5 cm; 10^8 cm$^{-3} \leq n_i = n_e \leq 10^{11}$ cm^{-3}; $T_e = T_i \sim 0.2$ eV; B = 1–7 kG) is produced by contact ionization of an alkali metal or alkali earth metal on an incandescently heated rhenium-coated tungsten hot plate. Barium was used because of the fortuitous electronic properties of the Ba^+ ion, allowing the use of laser-induced fluorescence (LIF) as a diagnostic. In Table 1 a comparison is made between suprauroral and Q machine experimental parameters. Note that for both plasma environments the ordering of ion and electron cyclotron/plasma frequencies are the same, that initial T_i, T_e are low, and that both plasmas are collisionless.

Laser-induced fluorescence techniques [*Stern and Johnson*, 1975; *Stern et al.*, 1981; *Hill et al.*, 1983] were used to measure ion velocity distributions at various angles relative to the externally imposed magnetic field. A single-frequency laser beam (ω_L, $\mathbf{k}_L$) excites optical transitions in barium ions which are measured by collection apparatus exterior to the plasma. This diagnostic is nonperturbing to the plasma and possesses good spatial, velocity, and temporal resolutions (1 mm^3, 3×10^3 cm/s, 1 μs, respectively). Ion velocity selection occurs according to the Doppler relation

$$\omega_L - \mathbf{k}_L \cdot \mathbf{v}_i = \omega_0 \tag{1}$$

where ω_0 is the natural Ba (II) transition frequency. As indicated by equation (1), velocity components along the axes perpendicular to $\mathbf{k}_L$ are not preferentially selected. Thus the measured distribution is

$$f_i(\mathbf{x}, v_x, t) = \int\int f_i(\mathbf{x}, \mathbf{v}, t)\, dv_y\, dv_z \tag{2}$$

where we have taken the laser beam to be in the x direction. A set of LIF velocity scans at various angles in the x-z plane contains information used to reconstruct the two-dimensional distribution via optical tomography [*Koslover and McWilliams*, 1986]. Spatially or temporally resolved phase

TABLE 1. Laboratory and Magnetospheric Parameters

	Q Machine	Suprauroral Region (Altitude ~2000 km)
Density	10^9–10^{11} cm^{-3}	10^1–10^3 cm^{-3}
B field	1–7 kG	0.15 G
Temperature	$T_e \sim T_i \sim 0.2$ eV	$T_e \sim T_i \sim 1$ eV
Mass	137 (Ba^+), 39 (K^+)	1 (H^+), 16 (O^+)
Length	133 (Cs^+)	4 (He^+)
Altitude	1 m, r = 2.5 cm	500–8000 km
	$\omega_{ce} > \omega_{pe} > \omega_{pi} > \omega_{ci}$	$\omega_{ce} > \omega_{pe} > \omega_{pi} > \omega_{ci}$
	LHW	
E_{rms}	5–500 V/cm	10–500 μV/cm
Wave $e\phi/T$	0 to >1	<1
$k_\perp/k_\parallel$	~500	~40–200
$v\phi$	$\sim v_{T_i}$	$> v_{T_i}$
$k_\perp \rho_i$	3–30	~1
Wave energy/ ion thermal energy	0.01–0.1	0.001–0.01
Wave/particle interaction time τ_{int}	$5 \times 10^3\ \omega_{LHR}^{-1}$	$3 \times 10^5\ \omega_{LHR}^{-1}$
Wave/particle interaction length	~1 m	~300 km
	EICW	
$k_\perp/k_\parallel$	~100	~10
Wave $e\phi/T$	~1	~1
	Ion Beam	
Beam energy U_{ib}	~4 eV	0–20 keV
Beam/target, n_{ib}/n_{io}	~0.5–1	~0.05–0.1
Beam temperature T_{ib}	0.2 eV	50–200 eV
Target temperature T_{it}	0.2 eV	2 eV

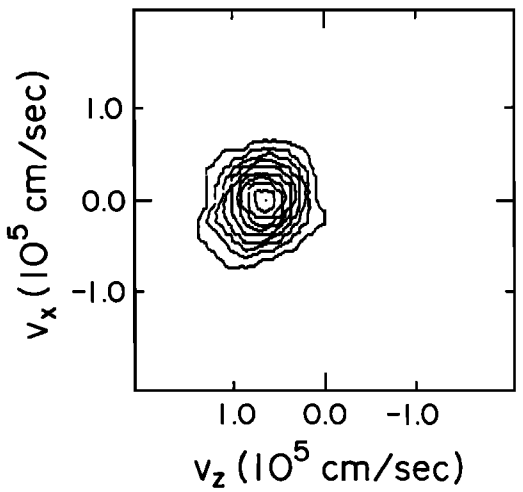

Fig. 2a

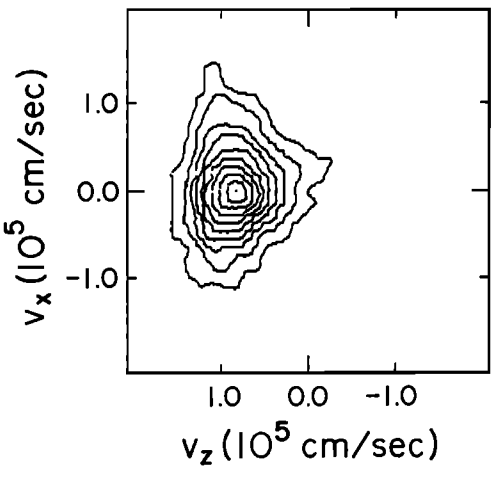

Fig. 2b

Fig. 2. (*a*) Contour plot of $f_i(v_x, v_z)$ for quiescent plasma conditions obtained by optical tomographic techniques (B = 6 kG, $n_i \approx 10^{10}$ cm^{-3}, $T_{i,e,\perp,\parallel} \approx 0.2$ eV). Outward from the center point, the contours represent decreasing percentages of maximum phase space density, i.e., 100%, 90%, 80%, $\cdots$, 20%, 10%. Note quiescent plasma has rough symmetry in v_x and v_z about center point (100%) and has net drift velocity $v_z \simeq 6.4 \times 10^4$ cm/s [from *Koslover and McWilliams*, 1986; *McWilliams and Koslover*, 1987]. (*b*) Phase space contour plot of $f_i(v_x, v_z)$ in the presence of current-driven EICW obtained by optical tomographic techniques. Contours have same definition as in Figure 2*a* [from *Koslover and McWilliams*, 1986; *McWilliams and Koslover*, 1987].

space reconstructions of a plasma system may be obtained from a series of discrete ion velocity distributions as described by *McWilliams and Sheehan* [1986].

3. Review of Current-Driven Electrostatic Ion Cyclotron Wave

In this section we review initial results linking EICW to ion conics [*McWilliams and Koslover*, 1987]. The EICW has been predicted and observed in the magnetosphere to result in perpendicular ion heating. In linear theory the current-driven EICW may be destabilized in a magnetic field by parallel electron drift ($v_d \geq 0.2\ v_{th}$) relative to the ion background. For the experimental collisionless Q machine plasma with $T_e \approx T_i$, for $k_\perp \gg k_\parallel$ and $k_{\perp\rho i} \approx 1$, the linear EICW dispersion relation is [*Drummond and Rosenbluth*, 1962; *Kindel and Kennel*, 1971]

$$\omega_{\text{EICW}} \simeq \omega_{ci}\left[1 + \frac{T_e}{T_i}\, e^{-s} I_1(s)\right] \tag{3}$$

where $I_1(s)$ is the modified Bessel function of order 1 and $s = k_\perp^2 \rho_i^2$. For the plasma parameters in this experiment, $\omega_{\text{EICW}} \approx 1.2\ \omega_{ci}$.

The current-driven EICW was destabilized and studied in a Q machine plasma column ($n_i = 5 \times 10^9$ cm^{-3}, B = 4 kG) as described by *McWilliams and Koslover* [1987] and as shown in Figure 1. Ion response to large-amplitude EICW ($e\phi/T > 1$) was examined using optical tomography [see *Koslover and McWilliams*, 1986; *McWilliams and Koslover*, 1987]. As a control (no EICW), Figure 2*a* shows the ion velocity distribution of the Q machine undisturbed, drifting, nearly Maxwellian plasma with an axial drift of about 6.4 × 10^4 cm/s, perpendicular ion temperature of about 0.17 eV, and parallel ion temperature of about 0.15 eV. The contours are lines of constant phase space density, f_i, in 10 equally spaced increments from 10% to 100% of $f_{i\max}$.

Alternating current excitation with a direct current bias generated electron flow and dc potentials [*Lang and Boehmer*, 1983] similar to those observed in the suprauroral region of the Earth's magnetosphere [*Mozer et al.*, 1977], although the sign of the potential is reversed. Figure 3 [*Lang*, 1984] shows contours of constant potential in the Q machine in the presence of the current-driven EIC instability.

The tomographic measurement was made at the current channel center and axially at about the equivalent Figure 3 position of z = 80 cm. The $v_x - v_z$ ion distribution function in the current channel is shown in Figure 2*b*, a v_y-integrated

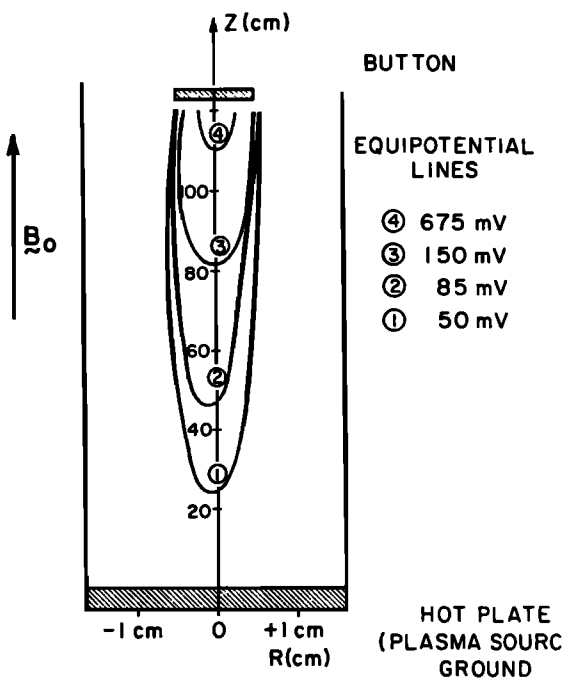

Fig. 3. Contours of constant dc potential near the biased button in the presence of the EICW [from *Lang*, 1984].

reconstruction from 16 scans. (Compare Figure 2*b* with Figure 2*a*.) Figure 2*b*'s distribution is similar to some magnetospheric observations [*Kintner and Gorney*, 1984] of ion conics. We conclude that a flaring B field is not always necessary to generate ion conics. In fact, simulations by *Borovsky* [1984] and others have shown that double layers might produce ion conics in the supraurorał region.

In conclusion, the current-driven EICW has been a popular candidate for TAI and conic formation. In theory, it is easily destabilized by field-aligned currents [*Kindel and Kennel*, 1971], and it is very efficient in ion heating. Experimentally, however, evidence is not conclusive for electron drift being a significant source of EICW and conics. Most in situ measurements suggest either of the following: (1) either electron drift or ion beams could be responsible (neglecting potential jumps) or (2) ion beams are responsible for EICW generation (see the next section). At altitudes above 5000 km, *Kintner et al.* [1979] showed that EICW are mostly correlated with upflowing ions rather than electron current. At lower altitudes, current-driven EICW faces the theoretical difficulty of requiring a high critical current. This condition might be met by filamentary current structures, as suggested by *Kintner et al.* [1979], but this awaits clear experimental verification in the supraurora. As an aside, in the laboratory, EICW have been generated by filamentary electron currents with widths r much less than ρ_i.

4. Ion Beam–Plasmas Interactions

Several electrostatic ion beam–plasma modes may be destabilized in the supraurorał region [*Perkins*, 1976; *Yamada et al.*, 1977; *Kaufmann and Kintner*, 1982, 1984]. The experiments reported here will focus on perpendicular ion energization and heating of both beam ions and background plasma ions resulting from parallel injection of an ion beam into a low-temperature target plasma. Two electrostatic modes were excited: the ion cyclotron cyclotron wave (ICCW) and the ion cyclotron drift wave (ICDW) [*Yamada et al.*, 1977]. The ICCW couples the beam cyclotron mode and the target plasma cyclotron mode and satisfies

$$\omega_{\mathrm{ICCW}} \approx \frac{u_b \omega_{cit} - u_t \omega_{cib}}{u_t + u_b} \tag{4}$$

$$k_{z(\mathrm{ICCW})} \approx \frac{\omega_{cit} + \omega_{cib}}{u_t + u_b} \tag{5}$$

where the subscripts t and b refer to the target and beam species, respectively, u is the species' drift relative to the laboratory frame (in meters per second), and ω_{ci} is the species' ion cyclotron frequency (in radians per second). Radial wavelengths are of the order of the beam diameter (≈7 mm), and parallel wavelengths are set by equation (5). Note that the wave is Doppler-downshifted from the ion cyclotron frequency ($f_{ci}(B = 5\ \mathrm{kG}) \approx 55$ kHz) by the plasma drift relative to the stationary RF probe such that $f_{\mathrm{ICCW}} \sim 10$ kHz, for the experimental conditions (4-V Ba^+ beam, $B = 5$ kG). The ICCW grows convectively in the parallel direction and absolutely in the radial direction. Lastly, wave energy does not propagate across the magnetic field ($(\partial\omega/\partial k_\perp) = 0$); therefore the mode is confined to the beam channel.

A second mode, the nonresonant ion cyclotron drift wave, was also observed. It is driven by the free energy associated with the pressure gradient at the beam edge. For reasons to be explained, its effects on ions were deemed minor in these experiments.

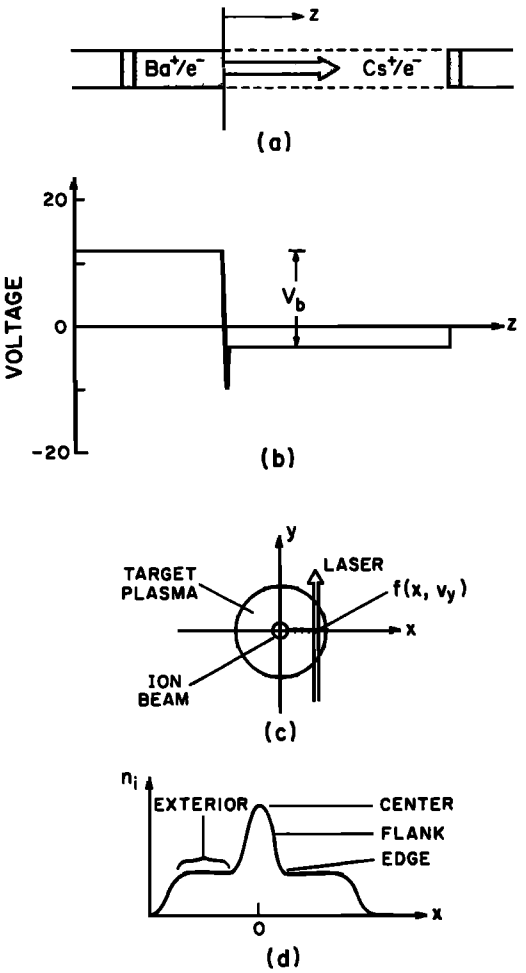

Fig. 4. (*a*) Schematic of double-plasma configuration. (*b*) Plasma and grid voltages for driving Ba^+ ion beam. (*c*) Cylindrical cross section of plasma column with laser beam. (*d*) Beam-plasma density profile.

Ion beams were driven in the Q machine using a double-plasma configuration [*Taylor et al.*, 1972], as shown in Figure 4*a*. The Q machine was operated double-ended with one Cs source and one Ba source, separated by an axially mobile screened annulus (OD = 10 cm, ID = 0.7 cm). The ion beam (diameter of 0.7 cm) was driven parallel to the magnetic field from a reservoir plasma (Ba^+/e^- in Figure 4*a*) into the 5-cm-diameter target plasma ($B = 5$ kG) by biasing the hot plates and beam aperture screen so as to establish a voltage differential between the two plasmas; for this experiment the voltage differential was 2 V. Also, the target plasma drifted toward the reservoir plasma with $v \simeq 1 \times 10^5$ cm/s. Adding the voltage differential to the effect of the target plasma drift, one calculates an effective beam energy of 4.2 eV relative to the target plasma.

The beam to target plasma density ratio could be varied from $0 \le (n_b/n_t) \le 1$. Various axial locations of the beam and target plasma were accessed by relocating the beam aperture axially. Also, this allowed driving either Cs^+ or Ba^+ beams through the LIF diagnostic region. In this way the heating of the beam ions could be investigated indepen-

dently of that of the background target plasma ions. Cesium and barium have similar mass ratios ($M_{Ba}/M_{Cs} = 137/133 \sim 1.03$); so this system may model aspects of H^+ or O^+ ion beams interacting with their respective plasmas.

In this discussion the z coordinate refers to the axial distance from the beam aperture in the direction of beam propagation. The conventions for x and y are revealed in a radial slice of the beam-plasma column (Figures 4*c* and 4*d*). Time scales for beam-plasma phenomena were estimated from values of axial position z and the beam drift velocity u_b through the relation $t = z/u_b$. The axial interval investigated in this work was 1 cm $\leq z \leq$ 30 cm.

Phase space reconstructions of these beam-plasma systems were made from multiple, discrete, spatially or temporally serial one-dimensional ion velocity distributions, $f(x, y = 0, z, v_y)$, as described by *McWilliams and Sheehan* [1986]. Integration has been performed over the orthogonal velocity coordinates. The cylindrical symmetry of the system, however, allows one to extrapolate these to $f(x, y, z, v_x, v_y)$; only v_z and t are lacking from the full distribution, $f(\mathbf{x}, \mathbf{v}, t)$. If one assumes constant beam drift velocity u_b, then z and t are coupled through the relation $t = u_b/z$. The diagrams presented span one velocity and one configuration space dimension on which contours of constant phase space density are plotted much as contours of constant elevation are plotted on topographical maps. The contours represent percentages of the maximum phase space density in the ambient plasma in the same manner as the results from optical tomography.

Beam ions and target plasma ions displayed substantial energization and heating perpendicular to the confining magnetic field in the presence of the ICCW. Ion phase space distortions and wave amplitude measurements were consistent with the spatial growth and decay of the ICCW. The ion beam parallel distribution function, also measured by LIF, did not show noticeable heating. This TAI distribution would, presumably, transform into a true ion conic were it to move along flaring magnetic field lines. In Figure 5*a*, four axially sequential x-v_y phase space density plots are presented for z = 1.9 cm, 5.4 cm, 8.6 cm, and 19.3 cm in the $Ba^+ \Rightarrow Cs^+/e^-$ system, depicting the spatial, time-averaged development of beam ions. For reference, z = 1.9 cm is an early stage in the beam development and z = 19.3 cm a later stage. Also, for comparison, Figure 5*b* depicts a numerically simulated x-v_y phase space plot of undisturbed, thermal Q machine ions. Comparing experimental to numerically simulated thermal ion phase space density plots, it is clear that the configuration space and velocity space extents of the experimental contours greatly exceed those of the simulation contours, indicating that nonballistic effects are operative in the beam development, i.e., perpendicular ion heating or energization. The energetic ions at ($x \approx 0$, $v_y > v_{ti}$), consisting of a 5% spike contour at $+v_y$ at z = 1.9 cm, and various island contours in the z = 1.9 cm and z = 5.4 cm plots, are believed to be generated, in part, by strong density gradient-driven drift waves or ion focusing by potential sheaths at the metallic aperture edge. The majority of the nonthermal phase space distortions, however, are consistent with ion response to the ICCW.

Consider Figure 5*a*. Nested phase space ellipses expand between z = 1.9 cm and z = 8.6 cm and then contract by z = 19.3 cm, indicating ions first increase perpendicular kinetic energy a factor of 3 over ambient thermal ions, then decrease a fraction of this. Over this axial interval the ICCW was the dominant wave mode. The de-energization of the beam ions (z = 19.3 cm) coincides roughly with the spatial heating of the target plasma as expected when beam energy is deposited in the target plasma. Also, by z = 19.3 cm only a vestige of the ICCW was seen. Note that there is an axially progressive loss of low-v_y contours (90%, 80% contours) caused by the progressive flattening of $f(v_y)$. This ion velocity space transport may be interpreted as wave heating of the beam ions, although temperatures cannot be ascribed to distributions so far from thermal equilibrium as these. The axial interval from the appearance to disappearance of the ICCW is consistent with estimates from quasi-linear velocity space diffusion of the parallel velocity coordinate of the beam as shown by *Yamada et al.* [1977].

Measurements of the beam ion parallel distribution function, $f(v_\parallel)$, revealed no significant parallel heating; thus one may infer that at maximum phase space extension, the ratio of perpendicular to parallel components of kinetic energy is roughly 3 : 1. Presumably, were this upstreaming TAI distribution to be found in the suprauroral region, adiabatic folding would create an ion conic from it.

Two ion beam–plasma instabilities, the ICCW and ICDW, were identified in and near the beam channel. The ICCW was the dominant mode for the experimental conditions in the $Ba^+ \Rightarrow Cs^+/e^-$ and $Cs^+ \Rightarrow Ba^+/e^-$ systems ($z \leq 25$ cm, ϕ_b = 4 V, $n_b/n_t \leq 1$). In Figure 6, wave spectra at various beam radial locations are presented for axial locations z = 2.7 cm and z = 16.7 cm in the $Cs^+ \Rightarrow Ba^+/e^-$ system. The ICCW, evident at z = 2.7 cm at $f \approx 10$ kHz, was confined to and fairly constant in amplitude across the beam radius. Near the beam center it broadened spectrally and shifted frequency, possibly due to interactions with broadband noise generated near the beam aperture and by differential Doppler shifting. The ICCW damped quickly with axial distance from the aperture; at z = 16.7 cm, only a vestige of the ICCW remains. The strength and axial location of this mode are consistent with the phase space distortions of the ion beam in Figure 5*a*. Ions, responding to wave fields, were energized in the perpendicular direction and extended radially beyond the beam channel. This behavior is similar to that documented for the current-driven EICW [*Stern et al.*, 1981; *McWilliams and Sheehan*, 1986]. The ICDW is evident in the bottom of Figure 6 at z = 16.7 cm at $f_{ICDW} \approx 80$ kHz in and radially beyond the beam channel. Its effect on beam ions is believed to have been minor, since its amplitude is much smaller than that of the ICCW over the axial interval of interest and also since its growth rate is smaller than that of the ICCW, as shown by *Yamada et al.* [1977].

An indication of the total perpendicular kinetic energy, KE_y, in the beam ions was made by taking the second velocity moment integration of each phase space distribution and then integrating with respect to x. In Figure 7, KE_y is plotted versus z normalized against the thermal expectation value, KE_0. Note that between z = 8.6 cm and z = 19.3 cm, the kinetic energy of the average beam ion decreases a factor of KE_0. Comparable energy was deposited in the target plasma over this interval. On the basis of Figure 7, one estimates about a 10–20% conversion efficiency of beam parallel kinetic energy into perpendicular kinetic energy. This is consistent with observations by *Yamada et al.* [1977] of quasi-linear ion beam slowing. A similar conversion efficiency for a 1-keV magnetospheric beam suggests per-

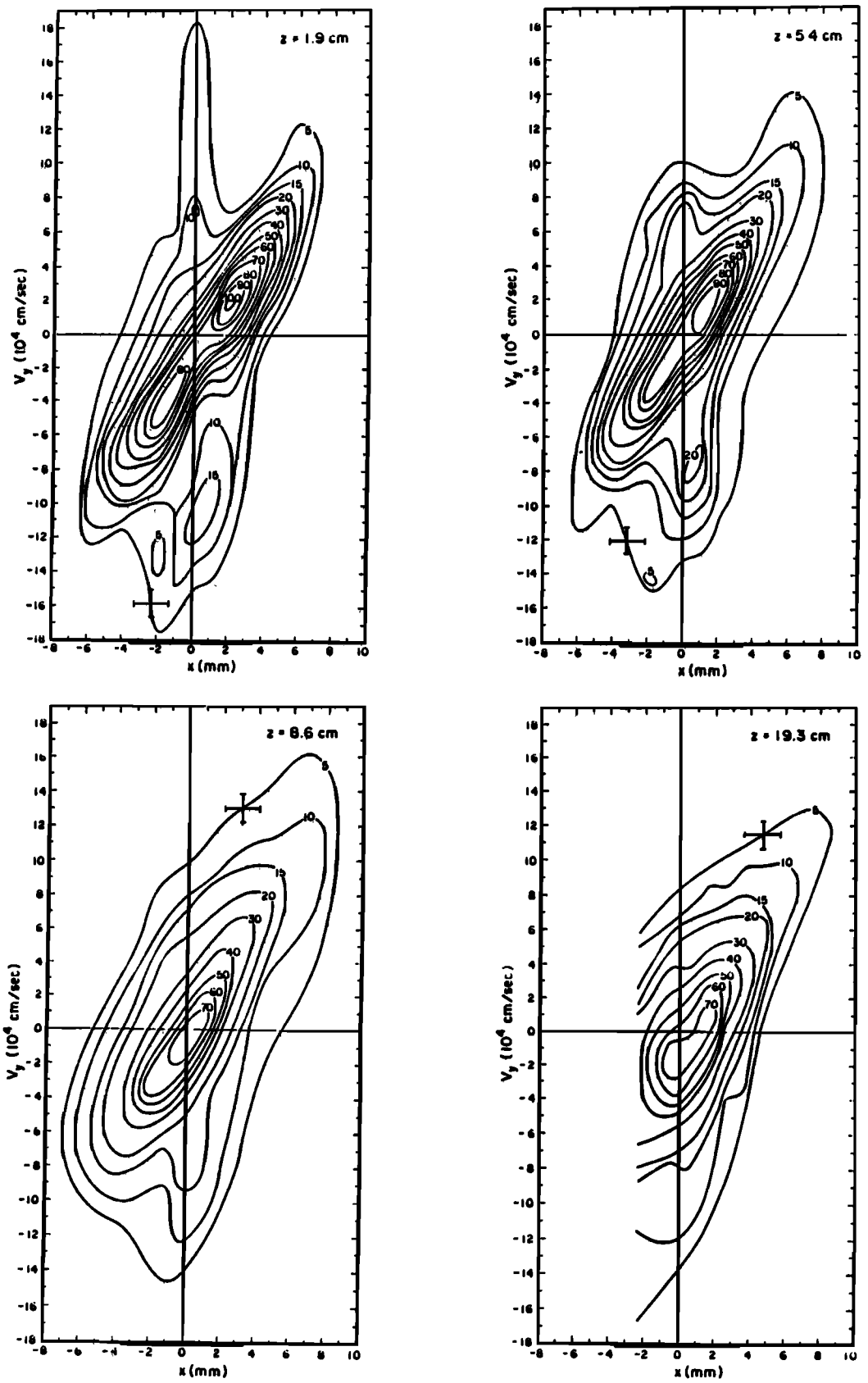

Fig. 5*a*

Fig. 5. (*a*) Axially sequential x-v_y ion phase space density plots (z = 1.9 cm, 5.4 cm, 8.6 cm, and 19.3 cm) for $Ba^+ \Rightarrow Cs^+/e^-$ system, depicting spatial development of beam ions in response to the ICCW. Plot at 19.3 cm is incomplete. (*b*) Numerically simulated phase space density plot for 0.2-eV quiescent state Q machine thermal ions for $z \geq 3$ cm. Contours numbered as to percentage of peak phase space density in ambient, undisturbed plasma. Bar below horizontal axis indicates extent of the beam source.

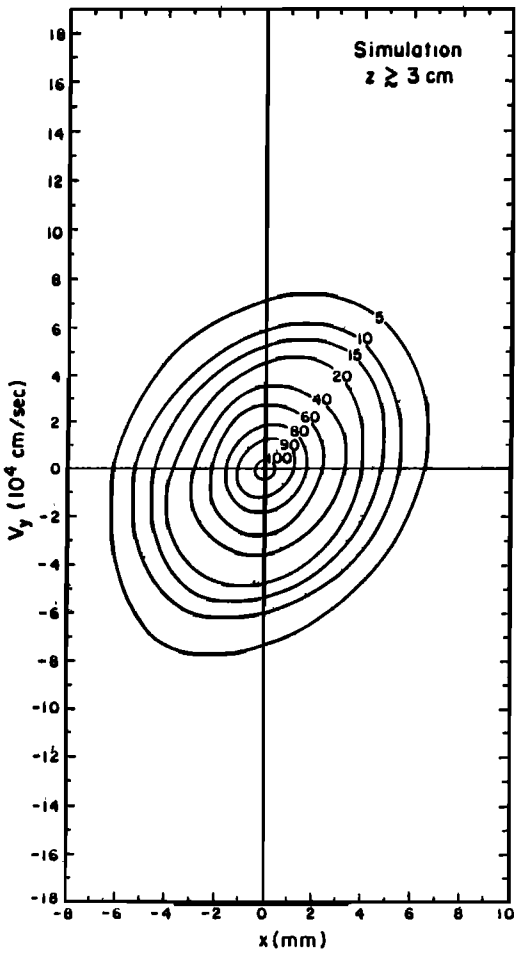

Fig. 5b

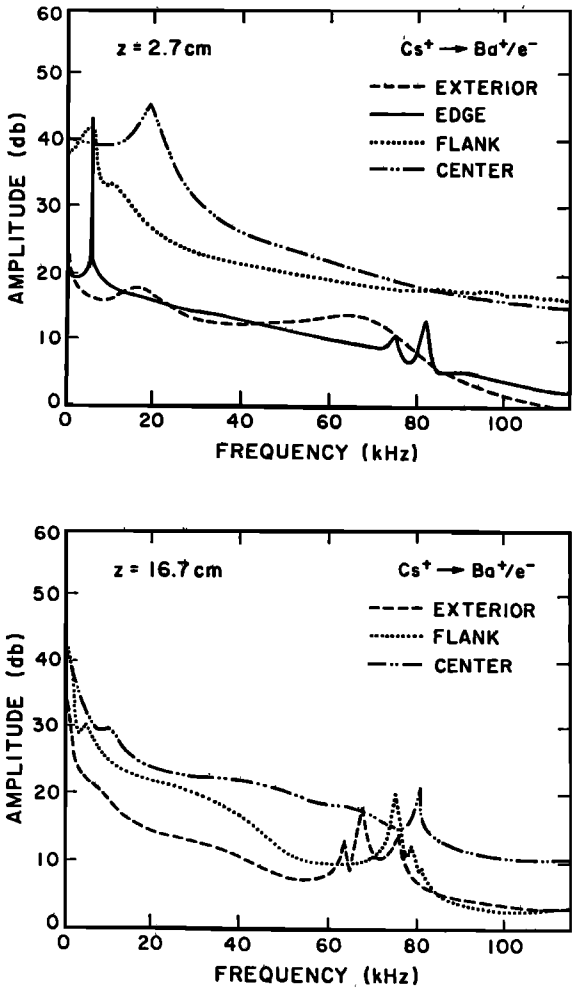

Fig. 6. Wave spectra at various radial locations in $Cs^+ \Rightarrow Ba^+/e^-$ system at axial locations $z = 2.7$ cm and $z = 16.7$ cm. ICCW, evident at $z = 2.7$ cm at $f \approx 10$ kHz, damps by $z = 16.7$ cm. ICDW is apparent at $f \approx 70$ kHz.

pendicular heating by 100 or 200 eV. This degree of heating has been measured by the S3-3 satellite for 1-keV ion beams at altitudes of 1 R_E [*Kintner et al.*, 1979].

Background target plasma ions displayed heating due to beam injection. Here, a Cs^+ beam was injected into a Ba^+/e^- plasma. In Figure 8, target plasma ion temperature is presented at various radial locations for three axial locations. Recall the target plasma is created approximately 80 cm upstream of, and drifts toward, the beam aperture such that large z values refer to early times in the target plasma development. For early times, $z \geq 35.2$ cm, the target plasma shows no heating. At later times the flank, edge, and center of the beam channel, however, display significant heating ($z = 16.7$ cm), approximately where the ICCW disappeared and the beam ion distended phase space ellipses (in Figure 5) collapsed. The flank and edge regions remained heated as the target plasma drifted to termination at the aperture plate. It is unclear why the center of the target plasma cooled near the beam aperture, although severe density depletion was observed there. Finally, as expected, the plasma exterior to the beam channel showed no heating, since the cyclotron modes were confined to the channel. In summary, beam ions were perpendicularly energized by an ion cyclotron mode (ICCW) to form an ion TAI velocity distribution, and to a lesser degree, the background plasma was perpendicularly heated in the region of the beam.

In the ionosphere and magnetosphere, upstreaming H^+, O^+, and He^+ ion beams are often accompanied by EICW [*Kaufmann and Kintner*, 1982; *Collin et al.*, 1984; *Kintner et al.*, 1979]. Data from the S3-3 spacecraft at about 1 R_E found that electrostatic hydrogen cyclotron waves (EHC) coincided with H^+ and O^+ ion beams in over 90% of studied

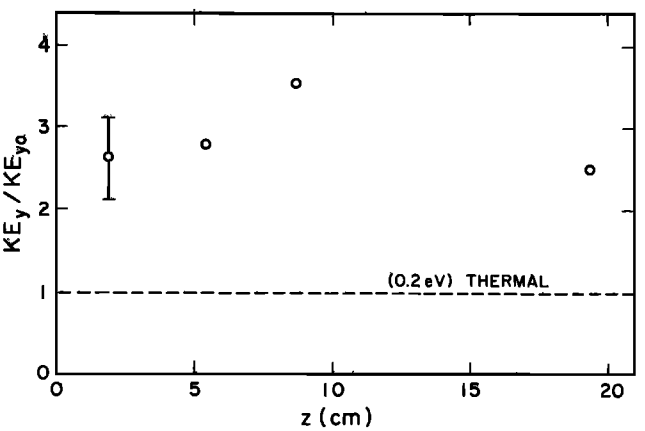

Fig. 7. KE_y/KE_{y0} versus z for $Ba^+ \Rightarrow Cs^+/e^-$ system. Circles, experimental results; dashed line, thermal ions.

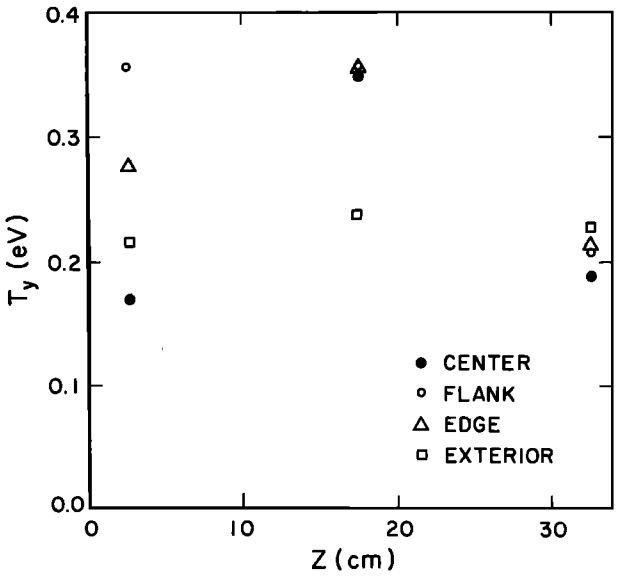

Fig. 8. Target plasma perpendicular temperature, T_y, versus z for various radial locations in $Cs^+ \Rightarrow Ba^+/e^-$ system.

events. To a lesser degree, statistical studies correlated perpendicular ion heating with EHC. Examples of ion conics coinciding with EHC were seen over large energy ranges: 90 eV (instrument threshold) to 6.2 keV and perhaps higher energies. Despite the statistical correlation between ion beams and EHC waves, however, the free energy source for the EHC being electrons cannot be ruled out; in fact, some S3-3 data supported electrons as possibly driving the EHC [*Kintner et al.*, 1979].

Comparisons are made in Table 1 between Q machine parameters and suprauroral ion beam–plasma conditions [*Kaufmann and Kintner*, 1982; *Kintner et al.*, 1979]. Both plasma systems are unstable to ion beam cyclotron modes when the beam velocity u_b is bounded by the ion sound speed C_s and the electron thermal velocity v_e, i.e., $C_s \ll u_b \ll v_e$. For a typical supraural ion beam–plasma environment with a 1-keV H^+ ion beam and a 3-eV H^+/e^- target plasma, one has $C_s = 1.7 \times 10^6$ cm/s, $u_b = 4.5 \times 10^7$ cm/s, and $v_e = 7.3 \times 10^7$ cm/s, thus marginally satisfying the instability criterion. For the present experiment, with a 4-eV ion beam (in the target plasma rest frame) and 0.2-eV Cs^+/e^- target plasma, one has $C_s = 3.7 \times 10^4$ cm/s, $u_b = 2.2 \times 10^5$ cm/s, and $v_e = 1.9 \times 10^7$ cm/s, thus satisfying the instability criterion.

It is interesting that similar ratios of $T_\perp/T_\parallel$ exist for both suprauroral beams and the present laboratory beam when the EICW is observed. From *Kaufmann and Kintner* [1982] and Table 1 of this text, one has $T_\perp/T_\parallel \simeq 148$ eV/71 eV $\sim$ 2.1, whereas for the present laboratory experiment, at maximum phase space extension, $T_\perp/T_\parallel \sim 3$. In the present experiment this ratio may be set by the velocity space diffusion of the parallel beam component. It is tempting to speculate that the same mechanism may be operative in the suprauroral region, particularly since the ratios of beam streaming energy to thermal energy are also similar for observed suprauroral beams and the present laboratory beams.

5. Perpendicular Ion Heating in the Presence of Lower Hybrid Waves

In this section, we review and develop initial findings linking LHW to ion heating [*McWilliams et al.*, 1986]. Lower hybrid waves have been proposed as a means to accelerate ions perpendicularly to the geomagnetic field. For our experimental conditions the propagation of LHW may be described well by cold plasma theory. Following *Schmidt* [1979], the dispersion relation for electrostatic oscillations for $ck/\omega \gg 1$, and $\omega_{ci} \ll \omega \ll \omega_{ce}$, is

$$\omega^2 = \frac{1}{1 + (\omega_{pe}/\omega_{ce})^2 + (k_\parallel/k_\perp)^2} \left(\omega_{pi}^2 + \frac{k_\parallel^2}{k_\perp^2} \omega_{pe}^2 \right) \tag{6}$$

The lower hybrid resonance frequency is defined by the limit of the perpendicular wave vector ($k_\perp \to \infty$):

$$\omega_{\mathrm{LHR}}^2 = \frac{\omega_{pi}^2}{1 + (\omega_{pe}/\omega_{ce})^2} \tag{7}$$

The resonant interaction of the ion distribution function $f_i(\mathbf{x}, \mathbf{v}, t)$ with broadband lower hybrid waves has been treated by *Chang and Coppi* [1981], using quasi-linear theory.

Lower hybrid waves were launched with either broadband or narrow-band frequency spectra near the lower hybrid resonance frequency (RF) with control over bandwidth, center frequency, and wave amplitude [see *McWilliams and Koslover*, 1987]. Excitation was by a 12-cm 8-ring cylindrical antenna [*Bellan and Porkolab*, 1976] coaxial with the plasma column (Figure 9). All of the rings were driven in parallel. Under such circumstances, RF was found everywhere in the plasma column, and resonance cones were not evident. Narrow-band and broadband RFs were found to produce similar ion heating effects. Narrow-band excitation refers to sinusoidal antenna excitation (e.g., 1 MHz ± ~5 kHz), whereas broadband excitation refers to a roughly Gaussian noise spectrum centered on a particular frequency (e.g., 1.8 MHz ± ~250 kHz). At higher frequencies ($\omega \geq 10\ \omega_{th}$), wavelength measurements on LHW resonance cones verified the dispersion relation, equation (6).

As described previously in the work of *McWilliams et al.* [1986], perpendicular ion heating in the presence of LHW was measured at the plasma column center, downstream from the antenna for various excitation frequencies and power levels [*McWilliams et al.* [1986]. For the plasma

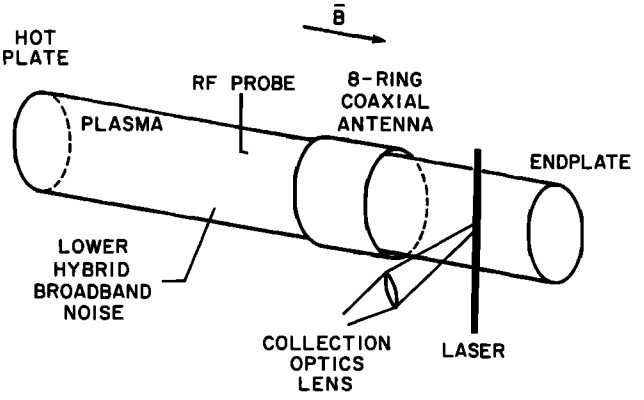

Fig. 9. Schematic of LHW experiment.

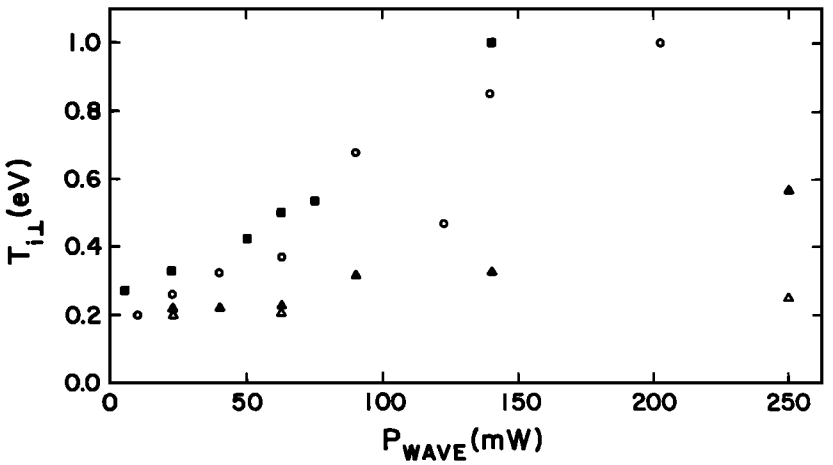

Fig. 10. $T_{i\perp}$ versus input LHW broadband RF power. Squares, f_{center} = 3.4 MHz; circles, f_{center} = 2.5 MHz; solid triangles, f_{center} = 2.0 MHz; open triangles, f_{center} = 1.5 MHz.

excited by broadband LHW, Figure 10 shows $T_{i\perp}$ versus estimated wave power, at band center frequencies of 1.5, 2.0, 2.5, and 3.4 MHz. For this plasma, $f_{pi} \sim 1.8$ MHz. As expected, below ω_{pi} there is little perpendicular heating observed. As the frequency is increased through ω_{LHR} and approaching $2\omega_{pi}$, increased ion heating is observed. The maximum temperature observed was up to 6 times the initial temperature. Parallel distribution functions exhibited a change of 25% or less in $T_{i\|}$ over the range of parameters studied here. Therefore one may infer that, at maximum heating, values of $T_\perp/T_\|$ up to about 5 and that folding of similar suprauroral distributions could result in conics. In addition to heating, many of the distributions displayed non-Maxwellian tails. The maximum energy of ions in these tails (corresponding to a signal level of about 2% of the distribution peak) was about 25 times the initial ion thermal energy.

Except at very low signal levels, the probe spectra possess features not seen in the antenna input spectra. Figure 11 depicts probe frequency spectra and corresponding ($f_i(v_\perp)$ for f = 1.8 MHz broadband antenna excitation at various antenna voltages. Clearly evident in the f spectra are multiples of the fundamental input frequency. Also evident are waves at frequencies slightly below the fundamental. Both sinusoidal excitation and broadband excitation of the antenna resulted in generation of multiple harmonics of the input signal. This harmonic generation is believed due to a nonlinear coupling between the antenna and the plasma [*Skiff et al.*, 1984], rather than an indication of a nonlinear process within the plasma itself. Ion cyclotron harmonics, however, have been observed in the magnetosphere [*Temerin et al.*, 1979] and are a proven means of heating ions [*Ogawa et al.* , 1987; *Fukayama et al.* 1976]. In addition to multiple harmonics, waves were produced at fractions of the input frequency (see Figure 11). This is indicative of a genuine nonlinear plasma process, possibly the decay of the pump LHW into a daughter LHW and a heavily damped ion quasimode [*Porkolab*, 1977; *Wong and Ono*, 1981; *Koskinen*, 1985]. This hypothesis is consistent with the observed sudden fall off in spectral intensity at approximately 1 MHz, due to the daughter LHW being unable to propagate below f_{LHR}.

Ion velocity space transport in the presence of LHW was examined using LIF techniques. Large-amplitude ($e\phi/T > 1$) LHW were launched broadband with the center of the range at about $2\omega_{pi}$. Independent measurements of $f_i(v_\|)$ and $f_i(v_\perp)$ indicated heating up to $T_{i\perp}/T_{i\|} \sim 5$ depending on the input power level [*McWilliams et al.*, 1986].

In summary, substantial perpendicular ion heating and tail formation were observed in the presence of both broadband and narrow-band LHW for $\omega_{LHR} < \omega < 3\omega_{LHR}$. Spectra indicate the decay of antenna-launched pump waves into daughter LHW and lower-frequency waves, possibly heavily damped ion quasi-modes or broadband EICW. The ratio of wave energy to ion thermal energy is about 10 times greater for this experiment than for the suprauroral region. However, the time an ion spends in the interaction region of the suprauroral region (in terms of ω_{LHR}^{-1}) scales to nearly 100 times that of the laboratory. The relatively short length of the Q machine required that the ions be exposed to relatively stronger RF fields in order to study changes in $f_i(v_\perp)$.

More than one heating mechanism may be responsible for the observed results. Specifically, there may be both heating due to the decay-generated waves and resonant heating (consistent with $\omega \sim k_\perp v_i$) due to the pump waves. Heating

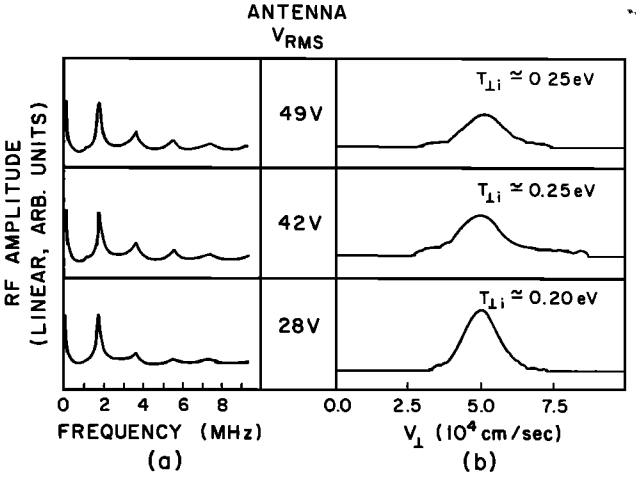

Fig. 11. Representative frequency spectra and corresponding ion velocity distributions, $f_i(v_\perp)$, for 1.8-MHz broadband antenna input at various excitation voltages.

of ions by EICW generated through the parametric decay of LHW has been seen in Q machines before [*McWilliams et al.*, 1983]. In that experiment the direct resonant interaction of LHW with $f_i(v_\perp)$ could be ruled out, since the wave phase velocity greatly exceeded the ion thermal velocity (because higher-frequency LHW were used). Additionally, the input power threshold for observation of parametric decay coincided with the threshold for perpendicular ion heating.

In contrast to the experiment just mentioned, in the experiment reported here, the wave phase velocity is probably not much greater than the ion thermal velocity. It has been suggested [*Kintner et al.*, 1986] that the relatively high phase velocity of lower hybrid waves in the suprauroral region may indicate that they may only play a secondary role of further heating hot ions that were initially heated by some other mechanism (e.g., EICW) to the point that they could effectively couple with LHW. Experimental results from the MARIE sounding rocket experiment [*Kintner et al.*, 1986] show a strong correlation between the presence of waves near ω_{LHR} and energy flux to the rocket's ion detectors. The approximately linear correlation extends across a factor of 10^2 in both the ion energy flux and the electric field amplitude. This observation favors the model by *Chang and Coppi* [1981] of ion conic formation by interaction of ions with broadband LHW.

Computer simulations [*Retterer et al.*, 1983, 1986] of ion interaction with LHW indicate tail formation, but very little bulk heating. This is contrary to the observations of the present experiments. *Koskinen* [1985], however, has suggested that the RF amplitude of LHW in the suprauroral region may be sufficient to excite the parametric decay processes. Decay products are indicated in these experiments.

In a search for plasma processes associated with conics, *Kintner and Gorney* [1984] examined data from the S3-3 satellite and found evidence possibly indicating that electrostatic LHW can lead to conics. Starting from the assumption that ion conics were caused by perpendicular ion heating, they searched for data simultaneously displaying broadband plasma waves and ion heating. They discovered one example: waves at the LHW resonance and above accompanied by perpendicular ion heating. At resonance, amplitudes were 0.2–6 mV/m (rms) for 800–1400 Hz, and for above LHR, wave amplitudes were generally below 10 mV/m, but briefly reached 30 mV/m (rms). Unfortunately, wave identification was not conclusive, since satellite probes could not discriminate between electrostatic and electromagnetic waves and since the O^+ ion cyclotron mode, if present, would have been Doppler-shifted below instrument detection and, hence, could not be ruled out as a heating mechanism. Assuming that electrostatic lower hybrid waves were detected by S3-3, one may compare Figure 3 from *Kintner and Gorney* [1984] with values from LHW-heated distributions in this paper. One notes similar ratios $v_\perp/v_\parallel \sim 2$–5 for both ion distributions.

6. SUMMARY

This paper has presented and reviewed ongoing laboratory experiments that simulate processes that could lead to ion conic formation in the terrestrial suprauroral region. A review was made of ion conic formation in the presence of current-driven EICW and an associated dc potential structure. Although equipotentials with a similar topology exist in the suprauroral region, the electric fields are in the opposite direction in comparison with the present experiment. However, the perpendicular heating of the ions by the EICW, as observed here, in combination with diverging magnetic field lines would lead to ion conics.

Ion beam-plasma systems displayed perpendicular ion energization of beam and target plasma ions in the presence of the ICCW. Beam ions did not show heating in the parallel direction; therefore one may infer the production of ion preconics by the ICCW. Perpendicular ion energization and ion conics accompanied by ion beam modes have been predicted or observed in the magnetosphere by a number of workers. Ion response to ion and electron beam cyclotron modes (EICW and ICCW) was found to be similar.

Substantial perpendicular ion heating ($T_{i\perp}$ up to 5 times $T_{i\perp 0}$) and non-Maxwellian tails in $f_i(v_\perp)$ were observed in the presence of broadband or narrow-band antenna-launched LHW in a frequency range near and above ω_{LHR}. Evidence of parametric decay was seen in the wave spectra.

Several mechanisms leading to ion conic formation appear to be possible, based on satellite measurements, theoretical models, and these laboratory experiments. This is not surprising, however, given the menagerie of waves, plasma species, and environments present in the suprauroral region.

Acknowledgments. We gratefully acknowledge useful discussions with N. Rynn, H. Böhmer, and N. Wolf of Dickinson College, Pennsylvania. We appreciate the laboratory assistance of J. Bowles and the engineering support provided by S. Roe and D. Parsons. This work was supported by National Science Foundation grants ATM-8716631 and PHY-8606081.

The Editor thanks M. A. Temerin and another referee for their assistance in evaluating this paper.

REFERENCES

Ashour-Abdalla, M., H. Okuda, and C. Z. Cheng, Acceleration of heavy ions on auroral field lines, *Geophys. Res. Lett.*, *8*, 795, 1981.

Bellan, P. M., and M. Porkolab, Experimental studies of lower hybrid wave propagation, *Phys. Fluids*, *19*, 995, 1976.

Böhmer, H., J. P. Hauck, and N. Rynn, Ion-beam excitation of electrostatic ion cyclotron waves, *Phys. Fluids*, *19*, 450, 1976.

Borovsky, J. E., The production of ion conics by oblique double layers, *J. Geophys. Res.*, *89*, 2251, 1984.

Cartier, S. L., N. D'Angelo, and R. L. Merlino, Electrostatic ion-cyclotron waves in a nonuniform magnetic field, *Phys. Fluids*, *28*, 3066, 1985.

Cattell, C., The relationship of field-aligned currents to electrostatic ion cyclotron waves, *J. Geophys. Res.*, *86*, 3641, 1981.

Cattell, C., R. Lysak, R. B. Torbert, and F. S. Mozer, Observations of differences between regions of current flowing into and out of the ionosphere, *Geophys. Res. Lett.*, *6*, 621, 1979.

Chang, T., and B. Coppi, Lower hybrid acceleration and ion evolution in the suprauroral region, *Geophys. Res. Lett.*, *8*, 1253, 1981.

Collin, H. L., R. D. Sharp, E. G. Shelley, and R. G. Johnson, Some general characteristics of upflowing ion beams over the auroral zone and their relationship to auroral electrons, *J. Geophys. Res.*, *86*, 6820, 1981.

Collin, H. L., R. D. Sharp, and E. G. Shelley, The magnitude and composition of the outflow of energetic ions from the ionosphere, *J. Geophys. Res.*, *89*, 2185, 1984.

Drummond, W. E., and M. N. Rosenbluth, Anomalous diffusion arising from microinstabilities in a plasma, *Phys. Fluids*, *5*, 1507, 1962.

Fukayama, A., H. Momota, and R. Itatani, Stochastic acceleration by an electrostatic wave near ion cyclotron harmonics, *Res. Rep. Inst. Plasma Phys. Nagoya Univ.*, *IPPJ-259*, 15, 1976.

Ghielmetti, A. B., R. G. Johnson, R. D. Sharp, and E. G. Shelley, The latitudinal, diurnal, and altitudinal distributions of upward-flowing energetic ions of ionospheric origin, *Geophys. Res. Lett.*, *5*, 59, 1978.

Gorney, D. J., A. Clarke, D. R. Croley, J. F. Fennel, J. M. Luhmann, and P. F. Mizera, The distribution of ion beams and conics below 8000 km, *J. Geophys. Res.*, *86*, 83, 1981.

Gorney, D. J., P. F. Mizera, and S. R. Church, On ion harmonic structure in auroral zone waves: The effect of ion conic damping on auroral hiss, *J. Geophys. Res.*, *87*, 10,479, 1982.

Gorney, D. J., Y. T. Chiu, and D. R. Croley, Trapping of ion conics by downward parallel electric fields, *J. Geophys. Res.*, *90*, 4205, 1985.

Hauck, J. P., H. Böhmer, N. Rynn, and G. Benford, Ion beam excitation of ion-cyclotron waves and ion heating in plasmas with drifting ions, *J. Plasma Phys.*, *19*, 237, 1978.

Hendel, H. W., M. Yamada, S. W. Seiler, and H. Ikezi, Ion-beam-driven resonant ion cyclotron instability, *Phys. Rev. Lett.*, *36*, 319, 1976.

Hill, D. N., S. Fornaca, and M. G. Wickham, Single frequency scanning laser as a plasma diagnostic, *Rev. Sci. Instrum.*, *54*, 309, 1983.

Horwitz, J. L., Conical distributions of low-energy ion fluxes at synchronouos orbit, *J. Geophys. Res.*, *85*, 2057, 1980.

Johnson, R. G., Energetic ion composition in the Earth's magnetosphere, *Rev. Geophys.*, *17*, 696, 1979.

Jones, D., Xe^+ -induced ion-cyclotron waves, *Space Res.*, *20*, 379, 1981.

Kaufmann, R. L., and P. M. Kintner, Upgoing ion beams, 1, Microscopic analysis, *J. Geophys. Res.*, *87*, 10,487, 1982.

Kaufmann, R. L., and P. M. Kintner, Upgoing ion beams, 2, Fluid analysis and magnetosphere-ionosphere coupling, *J. Geophys. Res.*, *89*, 2195, 1984.

Kindel, J. M., and C. F. Kennel, Topside current instabilities, *J. Geophys. Res.*, *76*, 3055, 1971.

Kintner, P. M., On the distinction between electrostatic ion cyclotron waves and ion cyclotron harmonic waves, *Geophys. Res. Lett.*, *7*, 585, 1980.

Kintner, P. M., and D. J. Gorney, A search for the plasma processes associated with perpendicular ion heating, *J. Geophys. Res.*, *89*, 937, 1984.

Kintner, P. M., and M. C. Kelley, Ion beam produced plasma waves observed by the $\delta n/n$ plasma wave receiver during the Porcupine experiment, *Adv. Space Res.*, *1*, 107, 1981.

Kintner, P. M., and M. C. Kelley, Plasma waves produced by the xenon ion beam experiment on the Porcupine sounding rocket, in *Artificial Particle Beams in Space Plasma Studies*, edited by B. Grandal, p. 199, Plenum, New York, 1982.

Kintner, P. M., and M. C. Kelley, A perpendicular ion beam instability: Solutions to the linear dispersion relation, *J. Geophys. Res.*, *88*, 357, 1983.

Kintner, P. M., M. C. Kelley, R. D. Sharp, A. G. Ghielmetti, M. Temerin, C. Cattell, P. F. Mizera, and J. G. Fennell, Simultaneous observations of energetic (keV) upstreaming ions and electrostatic hydrogen cyclotron waves, *J. Geophys. Res.*, *84*, 7201, 1979.

Kintner, P. M., J. LaBelle, W. Scales, A. W. Yau, and B. A. Whalen, Observations of plasma waves within regions of perpendicular ion acceleration, *Geophys. Res. Lett.*, *13*, 1113, 1986.

Koskinen, H. E. J., Lower hybrid parametric processes on auroral field lines in the topside ionosphere, *J. Geophys. Res.*, *90*, 8361, 1985.

Koslover, R., and R. McWilliams, Measurement of multidimensional ion velocity distributions by optical tomography, *Rev. Sci. Instrum.*, *57*, 2441, 1986.

Lang, A., Large-amplitude electrostatic ion-cyclotron wave phenomena and their relationship to magnetospheric events, Ph.D. dissertation, Univ. of Calif., Irvine, 1984.

Lang, A., and H. Boehmer, Electron current disruption and parallel electric fields associated with electrostatic ion cyclotron waves, *J. Geophys. Res.*, *88*, 5564, 1983.

Lysak, R. L., Ion acceleration by wave-particle interaction, in *Ion Acceleration in the Magnetosphere and Ionosphere, Geophys. Monogr. Ser.*, vol. 38, edited by T. S. Chang, p. 261, AGU, Washington, D. C., 1986.

Lysak, R. L., M. K. Hudson, and M. Temerin, Ion heating by strong electrostatic ion cyclotron turbulence, *J. Geophys. Res.*, *85*, 678, 1980.

McWilliams, R., and R. Koslover, Laboratory observation of ion conics by velocity-space tomography of a plasma, *Phys. Rev. Lett.*, *58*, 37, 1987.

McWilliams, R., and D. P. Sheehan, Experimental measurements of phase space, *Phys. Rev. Lett.*, *56*, 2485, 1986.

McWilliams, R., D. N. Hill, N. S. Wolf, and N. Rynn, Cross-field ion transport and heating due to parametric decay of lower hybrid waves, *Phys. Res. Lett.*, *50*, 836, 1983.

McWilliams, R., R. Koslover, H. Boehmer, and N. Rynn, Laboratory simulation of ion acceleration in the presence of lower hybrid waves, in *Ion Acceleration in the Magnetosphere and Ionosphere, Geophys. Monogr. Ser.*, vol. 38, edited by T. S. Chang, p. 245, AGU, Washington, D. C., 1986.

Miura, A., H. Okuda, and M. Ashour-Abdalla, Ion-beam-driven electrostatic ion cyclotron instabilities, *Geophys. Res. Lett.*, *10*, 353, 1983.

Mozer, F. S., C. W. Carlson, M. K. Hudson, R. B. Torbert, B. Parady, J. Yatteau, and M. C. Kelley, Observation of paired electrostatic shocks in the polar magnetosphere, *Phys. Rev. Lett.*, *38*, 292, 1977.

Mozer, F. S., C. A. Cattell, M. K. Hudson, R. L. Lysak, M. Temerin, and R. B. Torbert, Satellite measurements and theories of low altitude auroral particle acceleration, *Space Sci. Rev.*, *27*, 155, 1980.

Ogawa, Y., et al., Characteristics of ion Bernstein wave heating on the JIPP T-IIU tokamak, *Nucl. Fusion*, *27*, 1379, 1987.

Palmadesso, P. J., T. P. Coffey, S. L. Ossakow, and K. Papadopoulous, Topside ionosphere ion heating due to electrostatic ion cyclotron turbulence, *Geophys. Res. Lett.*, *1*, 105, 1974.

Perkins, F. W., Ion-streaming instabilities: Electromagnetic and electrostatic, *Phys. Fluids*, *19*, 1012, 1976.

Porkolab, M., Parametric instabilities due to lower-hybrid radio frequency heating of tokamak plasmas, *Phys. Fluids*, *20*, 2058, 1977.

Retterer, J. M., T. Chang, and J. R. Jasperse, Ion acceleration in the suprauroral region: A Monte Carlo model, *Geophys. Res. Lett.*, *10*, 583, 1983.

Retterer, J. M., T. Chang, and J. R. Jasperse, Ion acceleration by lower hybrid waves in the suprauroral region, *J. Geophys. Res.*, *91*, 1609, 1986.

Richardson, J. D., J. F. Fennell, and D. R. Croley, Jr., Observations of field-aligned ion and electron beams from SCATHA (P72-2), *J. Geophys. Res.*, *86*, 10,105, 1981.

Rynn, N., Current-induced effects in an alkali metal plasma, *Phys. Fluids*, *5*, 634, 1962.

Rynn, N., Improved quiescent plasma source, *Rev. Sci. Instrum.*, *35*, 40, 1964.

Rynn, N., and N. D'Angelo, Device for generating a low temperature highly ionized cesium plasma, *Rev. Sci. Instrum.*, *31*, 1326, 1961.

Rynn, N., D. R. Dakin, D. L. Correll, and G. Benford, Ion heating by the current-driven electrostatic ion-cyclotron instability, *Phys. Rev. Lett.*, *33*, 765, 1974.

Schmidt, G., *Physics of High Temperature Plasmas*, Academic, San Diego, Calif., 1979.

Shelley, E. G., Heavy ions in the magnetosphere, *Space Sci. Rev.*, *23*, 465, 1979.

Singh, N., and R. W. Schunk, Energization of ions in the auroral plasma by broadband waves: Generation of ion conics, *J. Geophys. Res.*, *89*, 5538, 1984.

Singh, N., R. W. Schunk, and J. J. Sojka, Energization of ionospheric ions by electrostatic hydrogen cyclotron waves, *Geophys. Res. Lett.*, *8*, 1249, 1981.

Skiff, F. N., K. L. Wong, and M. Ono, Harmonic generation and parametric decay in the ion-cyclotron frequency range, *Phys. Fluids*, *27*, 2205, 1984.

Stern, R. A., and J. A. Johnson, Plasma ion diagnostics using resonant fluorescence, *Phys. Rev. Lett.*, *34*, 1548, 1975.

Stern, R. A., D. N. Hill, and N. Rynn, Azimuthal coherent ion ring beam generation in unstable magnetized plasmas, *Phys. Rev. Lett.*, *47*, 792, 1981.

Taylor, R. J., K. R. MacKenzie, and H. Ikezi, A large double plasma device for plasma beam and wave studies, *Rev. Sci. Instrum.*, *43*, 1675, 1972.

Temerin, M., M. Woldorff, and F. S. Mozer, Nonlinear steepening of the electrostatic ion cyclotron wave, *Phys. Rev. Lett.*, *43*, 1941, 1979.

Temerin, M., C. Cattell, R. Lysak, M. Hudson, R. B. Torbert, F. S. Mozer, R. D. Sharp, and P. M. Kintner, The small-scale structure of electrostatic shocks, *J. Geophys. Res.*, *86*, 11,278, 1981.

Whalen, B. A., W. Bernstein, and P. W. Daley, Low altitude acceleration of ionospheric ions, *Geophys. Res. Lett.*, *5*, 55, 1978.

Wong, K. L., and M. Ono, Parametric decay of lower-hybrid waves in the ACT-1 toroidal device, *Phys. Rev. Lett.*, *47*, 842, 1981.

Yamada, M., S. Seiler, H. W. Hendel, and H. Ikezi, Electrostatic ion cyclotron instabilities driven by parallel ion beam injection, *Phys. Fluids*, *20*, 450, 1977.

Yau, A. W., B. A. Whalen, A. G. McNamara, P. J. Kellogg, and W. Bernstein, Particle and wave observations of low-altitude ionospheric acceleration events, *J. Geophys. Res.*, *88*, 341, 1983.

R. Koslover, Voss Scientific, Albuquerque, NM 87108.

R. McWilliams, Department of Physics, University of California, Irvine, CA 92717.

D. P. Sheehan, Department of Physics, University of San Diego, San Diego, CA 92110.

(Received March 12, 1990;
revised July 13, 1990;
accepted August 27, 1990.)